A Steady-State SPICE Modeling of the Thermoelectric Wireless Sensor Network Node

Aneta Prijić, *Member, IEEE*, Miloš Marjanović, *Student Member, IEEE*, Ljubomir Vračar, *Member, IEEE*, Danijel Danković, *Member, IEEE*, Dejan Milić, and Zoran Prijić, *Member, IEEE*

***Abstract*— This paper presents results of the modeling of the thermoelectric wireless sensor network node realized with the aluminum core PCBs using SPICE. Static performances of the node are investigated under different thermal gradients, considering three commercial thermoelectric modules used inside the node as thermoelectric generators. Model parameters are derived from the datasheets of the modules and thermal and geometrical properties of the other node building elements. Simulation results are compared with those obtained by the full multiphysics numerical analysis and with experimental ones. An emphasis is put on the influence of the Peltier effect and Joule heating inside the thermoelectric generator on the model accuracy. It is demonstrated that the equivalent electro-thermal model of the node, in conjunction with electrical properties of the load, can be used for the estimation of harvesting efficiency of the nodes realized with different thermoelectric generators.**

***Index Terms*—Thermal energy harvesting; wireless sensor network node; thermoelectric generator; SPICE modeling.**

I. Introduction

WIRELESS sensor networks (WSNs) are widely used in broad applications. Nodes of such networks are often powered by harvesting energy in forms other than electrical that are present in their surroundings. One of the most common sources of energy is a thermal gradient, which is transformed into the electric voltage by thermoelectric generators (TEGs) [1]. These devices are incorporated into the WSN nodes along with appropriate electronics for power management and storage, sensors, microcontroller, as well as data transmitting devices. Preferable node design has a form of a small compact block, in order to provide its simple placement and rigidness when operated in an environment. Efficient operation of the node is primarily determined by the value of thermal gradient existing at its opposite sides. Besides that, it depends on the characteristics of the used TEG, thermal properties of the other building elements of the node and electrical properties of the incorporated electronics. Although, specially designed and manufactured TEGs enable the best harvesting performances, commercial thermoelectric modules, primarily aimed for heating/cooling can be used as TEGs under certain restrictions.

Characterization of TEGs, based on the data available from their datasheets and considering various operating conditions, can be analytical, experimental and carried out by multidimensional multiphysics or electrical circuit numerical simulations. Analytical models of TEGs are based on the system of nonlinear differential equations which can be solved in a closed form only for the specific applications by introducing some simplifying assumptions [2]. Experimental characterization of TEGs includes extraction of thermoelectric parameters with their temperature dependencies [1,3] or determination of the open-circuit output voltage and output power density [2]. Full electro-thermal numerical modelling of TEGs demands multidimensional multiphysics simulations using dedicated Finite Element Modeling (FEM) tools [4,5]. Equivalent electro-thermal models of TEGs developed for the SPICE-like simulators are very useful from an engineering point of view. They consist of mutually interacting electrical and equivalent thermal circuits of low or high complexity [1,2,6,7]. These TEG models are used in a conjunction with the equivalent thermal elements representing other building blocks of the node and characteristics of the electrical loading for quick estimation of the node performances.

In this paper the steady-state SPICE compatible model of thermoelectric harvesting WSN node is presented. The main goal was to construct the model that enables investigation of node performances when different commercial thermoelectric modules are used as thermoelectric generators i.e. power sources. Results are compared with full multiphysic numerical simulations and experimental measurements. Contributions of the effects that oppose the thermoelectric effect inside the TEG to the model accuracy are also considered.

II. TEG Model

The TEG consists of a number of thermoelectric pairs (N), electrically connected in a series and thermally arranged in a parallel. Each pair is formed by two elements made of conductive materials having thermoelectric properties and joined with the copper electrode. Electrical connection of the neighboring pairs is by another copper electrode. Free ends of

Aneta Prijić is with the Faculty of Electronic Engineering, University of Niš, Aleksandra Medvedeva 14, 18000 Niš, Serbia (e-mail: aneta.prijic@ elfak.ni.ac.rs).

Miloš Marjanović is with the Faculty of Electronic Engineering, University of Niš, Aleksandra Medvedeva 14, 18000 Niš, Serbia (e-mail: milos.marjanovic@ elfak.ni.ac.rs).

Ljubomir Vračar is with the Faculty of Electronic Engineering, University of Niš, Aleksandra Medvedeva 14, 18000 Niš, Serbia (e-mail: ljubomir.vracar@ elfak.ni.ac.rs).

Danijel Danković is with the Faculty of Electronic Engineering, University of Niš, Aleksandra Medvedeva 14, 18000 Niš, Serbia (e-mail: danijel.dankovic@ elfak.ni.ac.rs).

Dejan Milić is with the Faculty of Electronic Engineering, University of Niš, Aleksandra Medvedeva 14, 18000 Niš, Serbia (e-mail: dejanmilic00@ gmail.com).

Zoran Prijić is with the Faculty of Electronic Engineering, University of Niš, Aleksandra Medvedeva 14, 18000 Niš, Serbia (e-mail: zoran.prijic@ elfak.ni.ac.rs).

copper electrodes of the first and last pair in the structure form positive and negative electrical contacts of the generator, respectively. The ceramic plates, having a high thermal and negligible electrical conductivity, fit closely on the copper electrodes at opposite sides of the pairs and represent external sides of the TEG, as presented in Fig. 1. Thermoelectric elements are made of doped semiconductor alloys (p- and n-type) whose thermal conductivity $\lambda_p=\lambda_n=\lambda$ is low and the Seebeck coefficients are of the opposite signs (α_p is positive and α_n is negative).

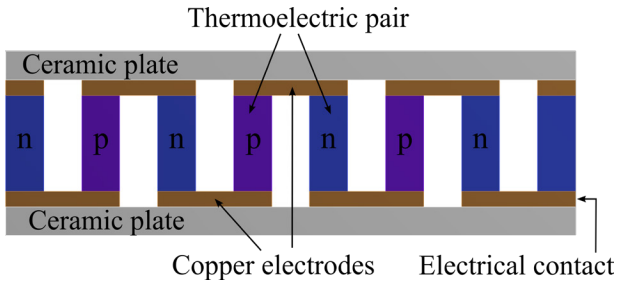

Fig. 1. Structure of the thermoelectric generator (front view).

Two sides of the TEG pairs have to be at different temperatures (T_{hot} and T_{cold}) in order to generate Seebeck voltage:

$$V_G = N\alpha_{pn}(T_{hot} - T_{cold}), \quad (1)$$

where $\alpha_{pn}=\alpha_p-\alpha_n$ represents the overall Seebeck coefficient. Internal resistance of the TEG equals the electrical resistance of all its elements:

$$R_{TEG} = \frac{2N\rho h}{A}, \quad (2)$$

where $\rho=\rho_n=\rho_p$ is electrical resistivity of thermoelectric materials, h is length and A the cross-sectional area of an individual element. By connecting load R_L to the TEG, an electrical circuit is formed enabling a flow of electrical current as shown in Fig. 2 [2]:

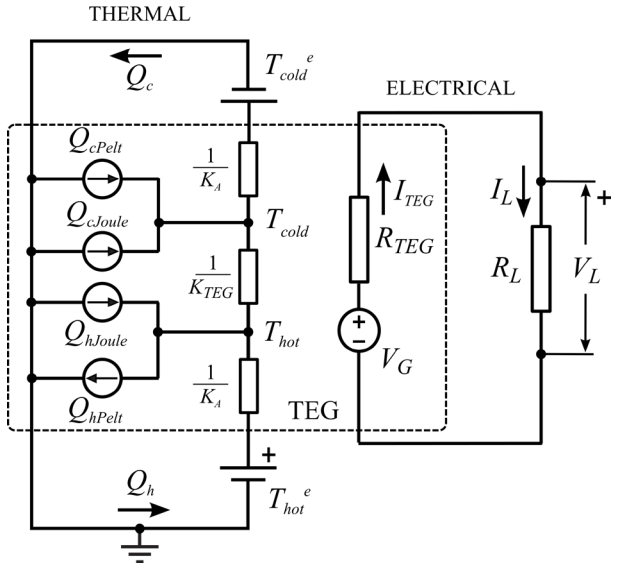

Fig. 2. Equivalent electro-thermal model of the TEG with the load and applied temperature difference.

$$I_L = I_{TEG} = \frac{V_G}{R_L + R_{TEG}}. \quad (3)$$

The current flow through the thermoelectric elements leads to the occurrence of the Peltier and Joule effects. The Peltier effect causes heat absorption of the rate Q_{cPelt} at the cold side and heat release of the rate Q_{hPelt} at the hot side of the pairs:

$$Q_{cPelt} = N\alpha_{pn}T_{cold}I_{TEG}, \quad (4)$$

$$Q_{hPelt} = N\alpha_{pn}T_{hot}I_{TEG}. \quad (5)$$

Also, Joule heating releases power i.e. heat rate which is evenly absorbed by hot and cold sides:

$$Q_{cJoule} = Q_{hJoule} = 0.5I_{TEG}^2R_{TEG} = 0.5V_{RTEG}I_{TEG}, \quad (6)$$

Heat conduction through the TEG elements from hot toward the cold side is governed by the Fourier law:

$$Q_{cond} = K_{TEG}(T_{hot} - T_{cold}), \quad (7)$$

where K_{TEG} represents the thermal conductance of all TEG elements:

$$K_{TEG} = \frac{2N\lambda A}{h}. \quad (8)$$

Overall heat rate absorbed at the hot side of the TEG elements Q_h and released to the environment at the cold side Q_c are balanced by the above mentioned heat rates according to the relations:

$$Q_h = N\alpha_{pn}T_{hot}I_{TEG} + K_{TEG}(T_{hot} - T_{cold}) - 0.5V_{RTEG}I_{TEG}, \quad (9)$$

$$Q_c = N\alpha_{pn}T_{cold}I_{TEG} + K_{TEG}(T_{hot} - T_{cold}) + 0.5V_{RTEG}I_{TEG}. \quad (10)$$

These heat rates also flow through the ceramic plates of the TEG according to the Fourier law:

$$Q_h = K_A(T_{hot}^e - T_{hot}), \quad (11)$$

$$Q_c = K_A(T_{cold} - T_{cold}^e). \quad (12)$$

They are related to the temperatures at TEG external sides T_{hot}^e and T_{cold}^e by the ceramic plate thermal conductivity:

$$K_A = \lambda_A\frac{A_{TEG}}{h_A}, \quad (13)$$

where λ_A is ceramic thermal conductance, A_{TEG} the external TEG area and h_A thickness of the ceramic plate.

Based on the analogy between quantities characteristic for the electrical and thermal domains, given in Table I, an equivalent electro-thermal network of the TEG can be constructed.

TABLE I
THE ANALOGY BETWEEN ELECTRICAL AND THERMAL QUANTITIES [8]

Electrical quantity	Voltage V (V)	Current I (A)	Resistance R (Ω)	Capacity C (F)
Thermal quantity	Absolute temp. T (K)	Heat rate Q (W)	Thermal resistance R_{th} (K/W)	Heat capacity C_{th} (J/K)

Topology of the network can be realized with distributed or lumped parameter values, depending on their distribution along the thermoelectric elements length [9]. The lumped parameter network, describing the TEG connected to the load R_L and subjected to the temperature difference $T_{hot}^e - T_{cold}^e$, is

shown in Fig. 2.

Interaction between two domains is established through voltage and current controlled generators (V_G, Q_{hPelt}, Q_{cPelt}, Q_{hJoule}, Q_{cJoule}). The overall Seebeck coefficient, electrical and thermal resistance can be considered as constant or temperature dependent parameters. The network from Fig. 2 can be analyzed using any SPICE like simulator for various boundary conditions. It is to be noted that this network is aimed for steady-state analysis where constant temperature difference at TEG sides and current dependent load are applied. Therefore, there are no capacitances that describe transient heat flow processes.

III. WSN Node Design and Model

The basic elements of the thermal energy harvesting wireless sensor network node are shown in Fig. 3. The commercial thermoelectric module is exploited as a thermoelectric generator to provide power for the node. Two external sides of the TEG are kept at different temperatures by exposing it to a heat source at the hot and by heat release to the ambient at the cold side. Temperature difference of a couple of tens degrees enables generation of the Seebeck voltage up to several hundreds of mV. This is insufficient for the operation of electronic devices, and the generated Seebeck voltage is introduced into the block for power management and storage, which enables continuous supply of the WSN node. Standard components of the node are different sensors and microcontroller for the acquisition of measured data, as well as a RF module for wireless data transmission.

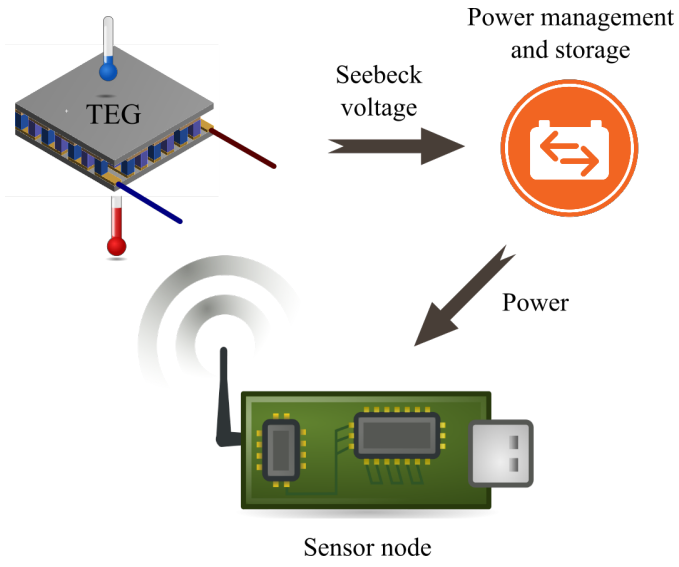

Fig. 3. Basic blocks of the thermal energy harvesting WSN node.

The investigated WSN node is realized as a stacked structure confined by two aluminum core PCBs with a mounted low-profile aluminum heatsink [10]. Its exploded view is shown in Fig. 4. An aluminum stand is placed between the bottom PCB and the TEG as a structural support to comply with the electronic components height. Bottom and top aluminum PCBs act as a heat collector for the hot and as an additional heat spreader for the cold side of the TEG, respectively. Thermally insulating foam fills space between the PCBs in order to reduce undesirable heat exchange. Thin layers of the thermal glue are used for parts joining to obtain good thermal contacts between them. All electrical components are placed on the inner side of the top PCB, except the temperature sensor which is on the inner side of the bottom PCB.

The main part of the power management and storage block is the step-up converter LTC3108 [11]. It is used with a 1:100 ratio transformer at the input, two 220 µF tantalum capacitors as a primary storage, and a 0.2 F supercapacitor as a backup storage. Data from the temperature sensor are collected by the low-power microcontroller PIC16F684 and transmitted over a 434 MHz RF module. The node is compact and provides reliable cold booting and prolonged autonomy when the temperature gradient extinguishes [10].

A model of the WSN node is built around the electro-thermal model of the TEG (Fig. 2) using LTSpice [12]. Corresponding elements of the thermoelectric model are given in Fig. 4. All added building elements of the node introduce equivalent thermal resistances connected at appropriate nodes of the network. Voltage generators *VThot* and *VTamb* are equivalents of the heat source and ambient temperatures, respectively. Port voltages *Thot* and *Tcold* represent temperatures at the hot and cold sides of the TEG pairs.

Dimensions and thermal properties of the node elements (aluminum PCBs, stand, thermal foam and glue, and heatsink) are listed in Table II. Value of the thermal resistance of each node structural element R_{thx} is determined by its length (thickness) h_x and cross-sectional area A_x, as well as thermal conductivity of its material λ_x:

$$R_{thx} = \frac{1}{K_{thx}} = \frac{h_x}{\lambda_x A_x}. \tag{14}$$

The foam has low thermal conductivity λ_{foam} and presents a thermally high resistive element on the path of the heat flow between PCBs:

$$R_{foam} = \frac{1}{K_{foam}} = \frac{h_{foam}}{\lambda_{foam}(A_{PCB} - A_{TEG})}. \tag{15}$$

This thermal resistance is the most critical parameter for the model accuracy since it represents a feedback loop of the electrical network. The value of thermal conductivity from Table II incorporates incomplete fulfillment of the space between PCBs and heat dissipation of the electronic components [10].

The voltage controlled voltage source (*VTEG*) models thermally generated voltage V_G given by (1), where value of the Seebeck coefficient is a temperature dependent parameter. The internal resistance of the TEG (*RTEG*) is also considered as temperature dependent. Values of these parameters are calculated for the mean temperature of the TEG (T_{hot}+T_{cold})/2, with T_0=298K as a reference temperature.

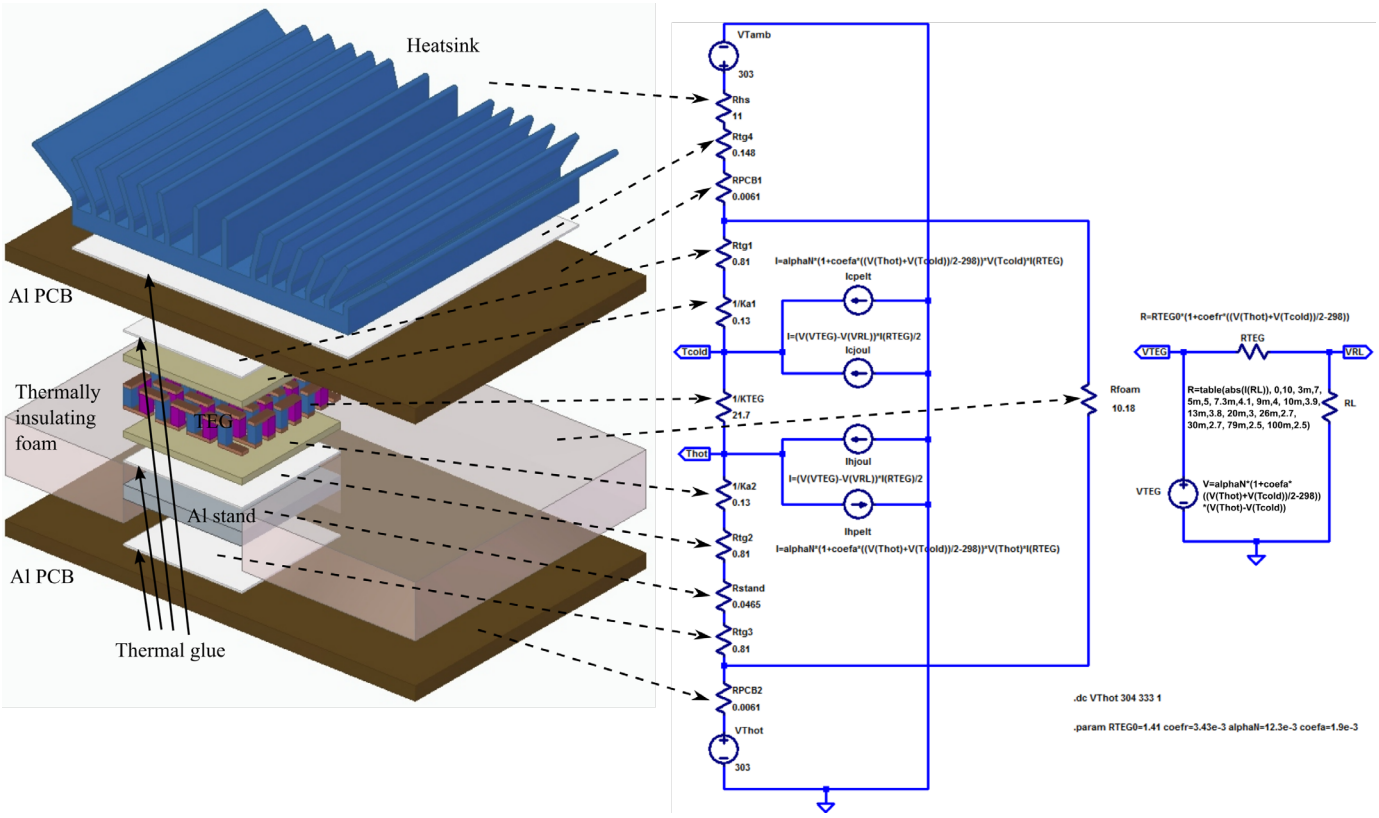

Fig. 4. Exploded view of the wireless sensor node and corresponding elements of the equivalent electro-thermal model.

TABLE II
DIMENSIONS AND THERMAL PROPERTIES OF THE WIRELESS SENSOR NODE ELEMENTS

Element / Property	Aluminum PCB	Stand	Thermal glue	Thermal foam	Heatsink
Thermal conductivity λ_x (W/mK)	153	153	1.1	0.4	209
Length (thickness) h_x (mm)	1.7	1.6	0.2	6.5	7.5 (fins)
Cross-sectional area A_x (mm^2)	1820	225	225/1225	1595	35×35 (base)
Thermal resistance R_{thx} (K /W)	$6.10 \cdot 10^{-3}$	0.0465	0.81/0.148	10.18	11

Load of the network is defined by the input resistance of the step-up converter LTC3108 when it charges primary and backup capacitances [11]. This value is in the interval (2.5-6) Ω depending on the load current value. It is modeled by a behavioral resistance using a look-up table with linear interpolation.

The arbitrary behavioral current generators (*Icpelt* and *Ihpelt*) model Peltier heat rates defined by (4) and (5) including a temperature dependent Seebeck coefficient. Contribution of the Joule effect given by (6) is modeled by generators *Icjoul* and *Ihjoul.*

IV. Simulation Results

The model is validated by simulation of the WSN node incorporating three different TEGs from two manufacturers [13,14]. Selected TEGs have internal resistances close to the impedance matched conditions (R_{TEG}=R_L), to enable operation around the maximum power transfer from the generator to the load. They are made of Bi_2Te_3 and differ in the thermoelectric pair number, material parameters, and dimensions of the thermoelectric element and ceramic plates. Values of the characteristic geometrical, electrical and thermal parameters of the considered TEGs, as well as values of the equivalent network elements are given in Table III.

Dependencies of the load voltage and load power on the temperature difference between the WSN node hot side and ambient for three TEGs are presented in Fig. 5 and Fig. 6, respectively.

TABLE III
CHARACTERISTIC GEOMETRICAL, ELECTRICAL AND THERMAL PARAMETERS OF THE CONSIDERED TEGS

Parameter (at T= 298K)	ET-031-10-20 (TEG1)	MCPE-071-10-15 (TEG2)	CP 08,31,06 (TEG3)
Number of thermoelectric pairs – N	31	71	31
External dimensions – (L×W×H) (mm)	15×15×4.3	20×20×3.8	12×12×3.3
Area of the TEG – A_{TEG} (mm^2)	225	400	144
Thermoelectric element dimensions – (l×w×h) (mm)	1×1×2.0	1×1×1.5	0.8×0.8×1.5
Ceramic plates thickness – h_A (mm)	0.75	0.75	0.60
Overall Seebeck coefficient – α_{pn} (μV/K)	396	396	378
Temperature coefficient of α_{pn} (1/K)	0.002	0.002	0.002
Thermoelectric element thermal conductivity – λ (W/m·K)	1.5	1.5	1.7
Ceramic plate thermal conductivity – λ_A (W/m·K)	25	25	25
Electrical resistivity of the thermoelectric element – ρ (μΩ·m)	11.4	11.4	10.6
Temperature coefficient of ρ (1/K)	0.0034	0.0034	0.0034
Ceramic plate thermal conductance– K_A(W/K)	7.50	13.33	6.3
Internal thermal conductance – K_{TEG} (W/K)	0.046	0.142	0.045
Internal electrical resistance – R_{TEG} (Ω)	1.41	2.43	1.54

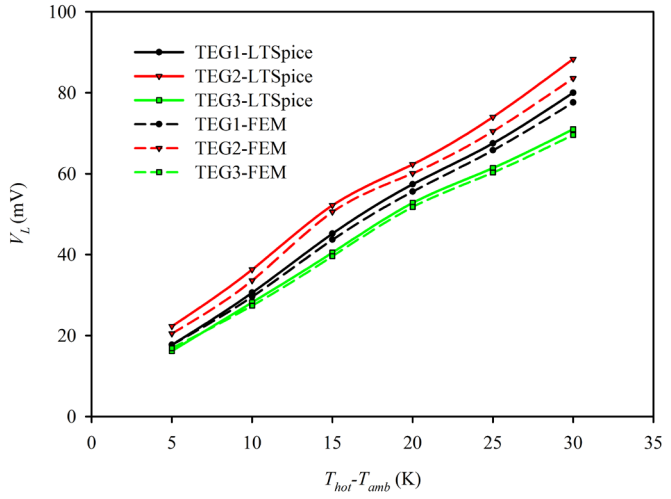

Fig. 5. Load voltage vs. temperature difference between the WSN node hot side and ambient for considered TEGs (LTSpice and FEM simulations).

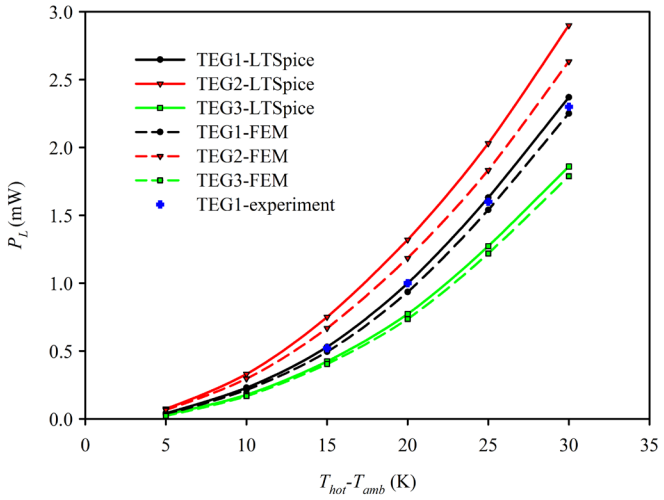

Fig. 6. Load power vs. temperature difference between the WSN node hot side and ambient for considered TEGs (LTSpice and FEM simulations and experimental values).

Obtained results are compared with the results of complete FEM simulations using ANSYS software [5]. Discrepancies are evident for higher temperature differences and for TEGs with a higher thermoelectric pair number and larger area. This is expected, since ANSYS simulations include additional internal thermal contact resistances and a thermal convection from node external sides to ambient. Overall, differences are less than 6% for voltage and 10% for power values. Moreover, obtained LTSpice simulation results are very close to the experimental measurements for TEG1. This verifies applicability of the presented model for characterization of different TEGs as parts of the considered WSN node.

Results from Figs. 5 and 6 indicate that TEG2, due to the higher N, enables the best harvesting efficiency, but it demands larger overall node dimensions. On the other hand, TEG3 is less efficient, but it has smaller external dimensions and can be used in nodes with demands for reduced size.

Equivalent electro-thermal model enables investigation of the influence of the effects that oppose Seebeck's and therefore reduce voltage generated by the TEG. Effect of the Joule heating is analyzed by removing the generators *Icjoul* and *Ihjoul* from the network. Results remain unchanged since this effect equally increases temperature of the hot and cold side of thermoelectric pairs and does not affect the temperature difference. However, since Peltier effect causes increase of the cold side and decrease of the hot side temperature, its influence is significant, as shown in Fig. 7. For TEG1 and TEG3 the difference is less than 15%, but for TEG2 this is as much as 50% due to the high number of thermoelectric pairs. This is the reason why analytical modeling of TEGs gives satisfactory results only for cases of fixed temperatures at TEG sides, where the influence of the Peltier effect is minimized [2,5].

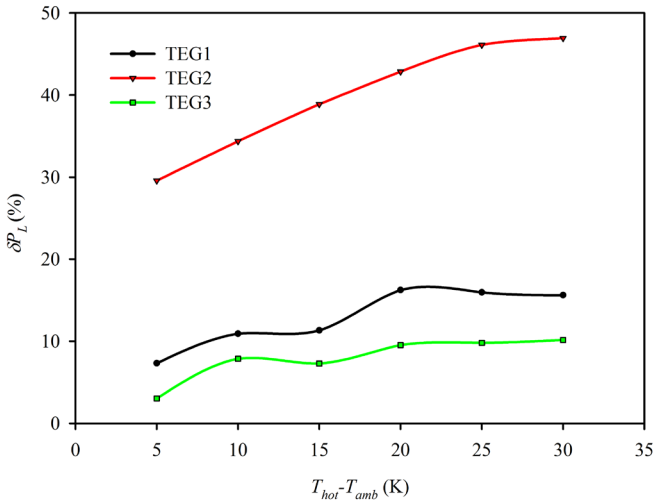

Fig. 7. Relative change of the load power vs. temperature difference between the WSN node hot side and ambient with neglected Peltier effect.

V. Conclusion

Fast and efficient simulation of the specific WSN node in a steady-state can be obtained using its equivalent SPICE compatible electro-thermal model. Determination of the equivalent network elements values demands knowledge of the geometrical, electrical and thermal parameters of the nodes building blocks, as well as electrical characteristics of the loading. Model is implemented for three thermoelectric modules used as generators inside the node. Obtained dependencies of the load voltage and power on the temperature difference are very close to the experimental and FEM simulation results. It is concluded that the Peltier effect occurring inside the TEG is significant for node efficiency, while the Joule effect can be neglected.

The model can be further improved by including transient heat exchange effects and using a complex electric circuit that describes the load.

Acknowledgment

This work was supported in part by the Serbian Ministry of Education, Science and Technological Development under Grant TR32026 and in part by Ei PCB Factory, Niš, Serbia.

References

[1] P. Dziurdzia, "Modeling and simulation of thermoelectric energy harvesting processes," in *Sustainable Energy Harvesting Technologies—Past, Present and Future*, Hampshire, U.K.: InTech, 2011.

[2] S. Dalola, M. Ferrari, V. Ferrari, M. Guizzetti, D. Marioli, A. Taroni, "Characterization of thermoelectric modules for powering autonomous sensors*", IEEE Trans. Instrum. Meas.*, vol. 58, pp. 99–107, Jan. 2009.

[3] M. Cernaianu, A. Cernaianu, C. Cirstea, A. Gontean, "Thermo Electrical Generator Improved Model," *Proc. 2012 International Conference on Power and Energy Systems*, Pune, India, Nov. 2012, pp. 343-348.

[4] O. Hogblom, R. Andersson, „Analysis of Thermoelectric Generator Performance by Use of Simulations and Experiments," *J. Elec. Mat.,* vol. 43, pp. 2246-2254, 2014.

[5] D. Milić, A. Prijić, Lj. Vračar, Z. Prijć, "Characterization of commercial thermoelectric modules for application in energy harvesting wireless sensor nodes", *Appl. Thermal Eng.*, vol. 121, pp. 74-82, Jul. 2017.

[6] M. Cernaianu, A. Gontean, „High-accuracy thermoelectrical module model for energy-harvesting systems*, IET Circuits Devices Syst*., vol. 7, pp. 114–123, Mar. 2013.

[7] M. Dousti, A. Petraglia, M. Pedram, "Accurate Electrothermal Modeling of Thermoelectric Generators," *Proc. 2015 Design, Automation & Test in Europe Conference & Exhibition*, Grenoble, France, March 2015, pp. 1603–1606.

[8] S. Lineykin, S. Ben-Yaakov, "Analysis of Thermoelectric Coolers by a Spice-Compatible Equivalent-Circuit Model", *IEEE Power Eletron. Lett,* vol. 3, pp. 63-66, Jun. 2005.

[9] D. Mitrani, J. Salazar, A. Turo, M. Garcıa, J. Chavez, "One-dimensional modeling of TE devices considering temperature-dependent parameters using SPICE", *Microelectronics Journal,* vol. 40, pp. 1398– 1405, 2009.

[10] A. Prijić, Lj. Vračar, D. Vučković, D. Milić, Z. Prijić, "Thermal energy harvesting wireless sensor node in aluminum core PCB technology," *IEEE Sensors J.*, vol. 15, pp. 337–345, Jan. 2015.

[11] "*LTC3108 ultralow voltage step-up converter and power manager*," Linear Technology Corporation, 2010, data sheet. [Online]. Available: http://www.linear.com.

[12] http://www.linear.com/solutions/ltspice.

[13] http://www.europeanthermodynamics.com/products/thermoelectric-modules/peltier-cooler.

[14] http://www.lairdtech.com/product-categories/thermal-management/thermoelectric-modules.